A lattice measuring method based on integral imaging technology[*]

ZHANG Xiao-dong (张晓东)******, **LI Suo-yin** (李锁印)**, HAN Zhi-guo** (韩志国)**, ZHAO Lin** (赵琳)**, LIANG Fa-guo** (梁法国)**, and WU Ai-hua** (吴爱华)

Hebei Semiconductor Research Institute, Shijiazhuang 050051, China

Aiming at the problem that the lattice feature exceeds the view field of the scanning electron microscope (SEM) measuring system, a new lattice measuring method is proposed based on integral imaging technology. When the system works, the SEM measuring system is equivalent to an integral image acquisition system. Firstly, a lattice measuring method is researched based on integral imaging theory. Secondly, the system parameters are calibrated by the VLSI lattice standard. Finally, the value of the lattice standard to be tested is determined based on the calibration parameters and the lattice measuring algorithm. The experimental results show that, compared with the traditional electron microscope measurement method, the relative error of the measured value of the algorithm is maintained within 0.2%, with the same level of measurement accuracy, but it expands the field of view of the electron microscope measurement system, which is suitable for the measurement of samples under high magnification.

With the development of semiconductor technology, microelectronic devices show a trend of high integration, small size and high performance. According to the international technology roadmap for semiconductors (ITRS), it is shown that from one technology node to the next, the key size of microelectronic devices is reduced at a rate of 0.7 times[1]. Therefore, precise control of key process parameters such as line width is the key to improving device performance. In the development process of microelectronic devices, domestic and foreign scientific research institutions usually use scanning electron microscope (SEM), atomic force microscope (AFM) and other line width measuring instruments to monitor line width parameters[2]. Due to the different measurement principles of the instruments, the measurement results are different. In order to solve the problem of inconsistent values, a micron-level lattice standard was developed to calibrate line width measurement instruments. However, in the case of high magnification, the grid characteristics of the micron-scale grid standard sample exceeds the field of view of the SEM measurement system, which affects the measurement capability of the instrument.

Integral imaging technology is based on optical principles to obtain three-dimensional information. It has the advantages of multiple viewing angles, simple structure, and high precision[3]. Hong Kong University of Science and Technology, Nankai University and other institutions have successively carried out research on stereo matching algorithms based on integral imaging technology to obtain the three-dimensional information of the object to be measured[4-6]. However, there is no relevant report on the application of integral imaging technology to micro-nano measurement technology. In order to obtain the information of the grid characteristics at high magnification, a grid measurement method is studied based on the principle of integral imaging. The algorithm cleverly combines related imaging principles and image processing technology, with high-precision measurement performance. Without using the electron microscope's own measurement function, the problem of electron microscope measurement under high magnification is solved.

Integral imaging is a technology that utilizes a lens array for information recording and reconstruction. The technology is mainly divided into two processes: the recording process and the reconstruction process[7]. The recording process is to optically encode the collected element images by using lenses of different viewing angles, and then store the three-dimensional information of the points to be measured in the form of plane information. The reconstruction process is to use computational integral imaging to resolve stored two-dimensional information[8].

Fig.1 shows the principle of integral imaging, take any point A, through point A' on the lens array, imaged as point A'' on the image acquisition system. Construct a Cartesian coordinate system on the lens array, where the Y-axis direction is vertically inward. Let unit (1,1) of the

lens array be that $A'(1, 1)=(0, 0, 0)$. From the optical knowledge, the relationship between the point A, the point $A'(i, j)$ on the lens array and the point $A''(i, j)$ on the image acquisition system is shown as

$$\begin{bmatrix} X_A \\ X_A \end{bmatrix} = \begin{bmatrix} X_{A'(i,j)} & X_{A''(i,j)} \\ X_{A'(i+a,j+b)} & X_{A''(i+a,j+b)} \end{bmatrix} \begin{bmatrix} 1+\dfrac{d}{g} \\ -\dfrac{d}{g} \end{bmatrix}, \tag{1}$$

$$\begin{bmatrix} Y_A \\ Y_A \end{bmatrix} = \begin{bmatrix} Y_{A'(i,j)} & Y_{A'(i,j)} \\ Y_{A'(i+a,j+b)} & Y_{A''(i+a,j+b)} \end{bmatrix} \begin{bmatrix} 1+\dfrac{d}{g} \\ -\dfrac{d}{g} \end{bmatrix}, \tag{2}$$

$$\Delta = X_{A''(i+a,j+b)} - X_{A''(i,j)} = aP(\frac{g}{d}+1). \tag{3}$$

The coordinate relationship between the lens array units is shown as

$$X_{A'(i+a, j+b)} = X_{A'(i+a, j)} = X_{A'(i, j)} + aP, \tag{4}$$

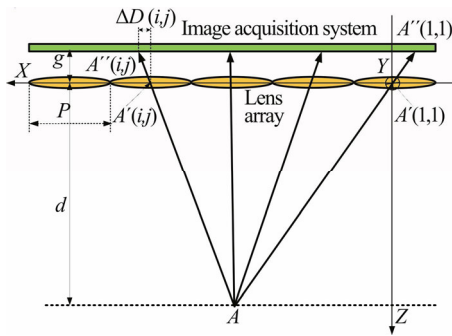$$Y_{A'(i+a, j+b)} = Y_{A'(i, j+b)} = X_{A'(i, j)} + bP. \tag{5}$$

Fig.1 Integral imaging principle

The coordinates of the point in the Cartesian coordinate system can be derived from Eqs.(1)—(5), which can be expressed as

$$X_A = (1+\eta)X_{A'(i, j)} - \eta X_{A''(i, j)}, \tag{6}$$

$$Y_A = (1+\eta)Y_{A'(i, j)} - \eta Y_{A''(i, j)}. \tag{7}$$

Among them, $\eta = d/g = aP/(X_{A''(i+a, j+b)} - X_{A''(i, j)} - aP)$. If $a=b=1$, then Eqs.(1)—(3) are transformed into the relationship between adjacent points on the lens array and adjacent image points of the acquired image[9].

As shown in Figs.2 and 3, the SEM measurement system is mainly composed of electronic optical system, vacuum system, scanning system, signal detection and amplification system, image display and recording system, and film transfer system. During the operation of the SEM system, the mechanical transmission system is responsible for the entry and exit of the sample. When the sample enters the electron microscope cavity, the electron beam emitted by the field source is irradiated onto the sample by two deflections, and the reflected secondary electrons are emitted to the electron detector through the optical lens, thereby completing the image acquisition of the electron microscope. In this paper, the

electron optical system, vacuum system, scanning system and signal detection amplification system are equivalent to an image acquisition system.
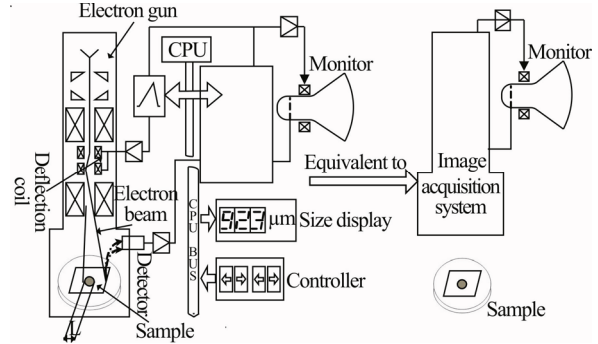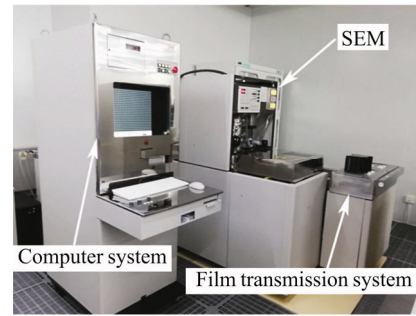

Fig.2 SEM measuring system

Fig.3 SEM measuring device

Select point A and point B on the surface to be tested. Based on the grid measurement algorithm, the relationship between point A and point B is shown as

$$\begin{bmatrix} X_A - X_B \\ Y_A - Y_B \end{bmatrix} = \begin{bmatrix} X_{A'(i,j)} - X_{B'(i,j)} & X_{A'(i,j)} - X_{B'(i,j)} \\ Y_{A'(i,j)} - Y_{B'(i,j)} & Y_{A'(i,j)} - Y_{B'(i,j)} \end{bmatrix} \begin{bmatrix} 1+\eta \\ -\eta \end{bmatrix}. \tag{8}$$

Then, the proportional relationship between parameters d and g can be determined as

$$\eta = \frac{d}{g} = \left| \frac{(X_A - X_B) - (X_{A'(i,j)} - X_{B'(i,j)})}{(X_{A'(i,j)} - X_{B'(i,j)}) - (X_{A''(i,j)} - X_{B''(i,j)})} \right|. \tag{9}$$

Point A and point B pass through the center of the lens unit in an idealized model. Therefore, $X_{A'(i, j)} = X_{B'(i, j)}$ on the (1,1) lens unit and the parameters d and g can be determined as

$$\eta = \frac{d}{g} = \left| \frac{(X_A - X_B)}{(X_{A''(i,j)} - X_{B''(i,j)})} \right|. \tag{10}$$

The sample used for system parameter calibration is the grid spacing standard sample, and the measurement value given is 3.00 μm±0.002 μm, which can be traced to the international metrology institute NIST. Therefore, it can be used as a standard sample for parameter calibration of the CD-SEM measurement system. In the parameter calibration process, a rectangular feature of the lattice standard is selected as the feature to be tested. When the magnification of the SEM is 80k, the lattice feature with a nominal value of 3 μm has exceeded the

field of view of the image acquisition system. At this time, $n \times n$ images are collected from the upper left corner of the lattice feature according to a fixed pitch in a manner of $n \times n$ square[10]. The size of n can be determined according to actual conditions. For the acquired images, the image stitching program is used for stitching, as shown in Fig.4. Then, the image is processed by the lattice measuring algorithm to complete the image acquisition system calibration and obtain the value η[11]. The average value of 6 calibrations is the η value, as shown in Tab.1.
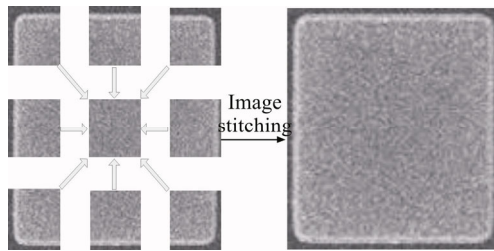

Fig.4 Stitched image of lattice standard

Tab.1 Calibration result of η value

Calibration times	η value	Average value
1	0.001 8	
2	0.001 9	
3	0.001 8	0.001 77
4	0.001 7	
5	0.001 7	
6	0.001 7	

The developed lattice standard with nominal values of 2 μm, 5 μm, and 10 μm were selected for measurement experiments, as shown in Fig.5. Firstly, select five representative areas of the sample upper, lower, left, right, and middle as the area to be tested, and number them. Secondly, the equivalent image acquisition system is used to collect the image features of the area to be tested, and the image is stitched[12]. Finally, based on the lattice measuring algorithm and the calibrated parameter values, the X-direction values of the five region grid features are obtained, as shown in Tab.1.
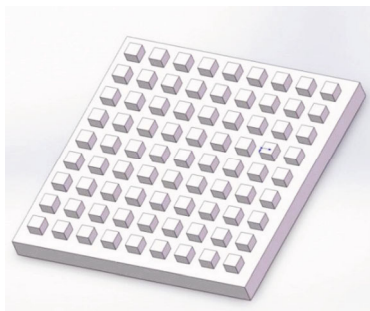

Fig.5 The developed lattice standard

In order to calculate the accuracy of the lattice meas-

uring algorithm, the developed lattice standard was measured using nano measuring machine (NMM) and used as a reference value. Among them, the measurement and positioning of the NMM is mainly realized by a laser interferometer of three axes, and the integral orthogonal positioning layout ensures that the orthogonal point of the measuring axis to the laser interferometer coincides with the measuring point of the sample to be tested, thereby the Abbe error is minimized, as shown in Fig.6. In addition, NMM's white light probe is based on the interference principle of a broad-spectrum light source, traceable to the laser wavelength, its measurement range is not less than 1 mm×1 mm, and the measurement uncertainty is 1 mm×2×10^{-7}L (k=2). Therefore, the NMM system measurement value is selected as the reference value, which has certain credibility and persuasive power.
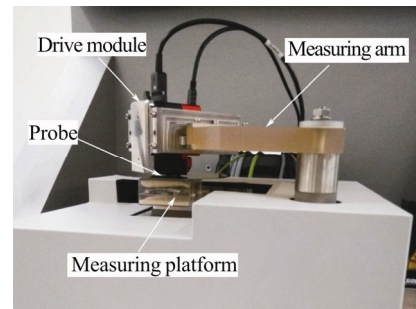

Fig.6 Nano-measuring machine

When the system works, the 2—10 μm lattice standards are placed on the NMM measuring platform in turn. The measuring platform is driven by the piezoelectric ceramics to perform nano-level precise movement, which ensures the rapid tracking and positioning of the lattice features. After scanning, the three-dimensional shape of the feature of the sample grid is reconstructed, and then the value of the grid is calculated. For the same reason, the 10 cycles of the lattice feature are selected, and the average value is taken as the lattice measurement value. In addition, using the NMM measurement as a reference value, the accuracy of the lattice measurement algorithm is calculated by calculating the relative error of the lattice measuring algorithm, as shown in Tab.2.

The experimental results show that the relative error of the lattice algorithm is maintained within 0.2%, which satisfies the experimental requirements, and proves the accuracy of the algorithm. The lattice measuring algorithm has the advantages of simple and no need to modify the instrument, and provides a theoretical method for solving the measurement problem of the high-magnification electron microscope.

In order to solve the problem that the lattice feature exceeds the field of view of the electron microscope under high magnification, based on the integral imaging technology and camera array principle, a lattice measuring method is proposed. Compared with the traditional

method, this method integrates the SEM measurement system without using the electron microscope measurement function, and effectively utilizes the image acquisition function of the electron microscope. Experiments

Tab.2 Characteristic measurement of lattice standard

Lattice standard	Serial number	Lattice measuring algorithm (μm)	NMM (μm)	Relative error
2 μm	1	1.999 6	1.997	0.13%
	2	1.999 1	1.997	0.11%
	3	1.999 0	1.997	0.10%
	4	1.999 5	1.997	0.13%
	5	1.999 4	1.997	0.12%
	Average	1.999 3	1.997	0.12%
5 μm	1	5.017	5.025	-0.16%
	2	5.019	5.025	-0.12%
	3	5.017	5.025	-0.16%
	4	5.022	5.025	-0.06%
	5	5.019	5.025	-0.12%
	Average	5.019	5.025	-0.12%
10 μm	1	10.023	10.009	0.14%
	2	10.019	10.009	0.10%
	3	10.024	10.009	0.15%
	4	10.019	10.009	0.10%
	5	10.024	10.009	0.15%
	Average	10.022	10.009	0.13%

show that this method not only expands the measurement field of view of SEM, but also provides a measurement method for SEM at high magnification. In addition, the research of lattice measuring algorithm, including edge detection algorithm and rectangle detection algorithm,

will be further studied and applied to lattice feature measurement to improve the standard accuracy of lattice standard.

References

[1]   Allan A, Journal of Applied Physics **86**, 045406 (2015).
[2]   Trache, A and Meininger G, Current Protocols in Microbiology **2** , Unit 2C.2 (2008).
[3]   Shen X, Markman A and Javidi B, Applied Optics **56**, D151 (2017).
[4]   Komatsu S, Markman A, Mahalanobis A, Chen K and Javidi B, Appl. Opt. **9**, D120 (2017).
[5]   Wang Y, Yang J, Liu L and Yan P, Acta Optica Sinica **39**, 1110001 (2019). (in Chinese)
[6]   Xiao X, Javidi B, Martinez-Corral M and Stern A, Applied Optics **52**, 546 (2013).
[7]   Chen X, Song X, Wu J, Xiao Y and Wang Y, Optics and Lasers in Engineering **136**, 106314 (2020).
[8]   Li D, Cheung C F, Ren M, Zhou L and Zhao X, Optics Express **22**, 25635 (2014).
[9]   Zhang H, Deng H, He M and Wang Q, Applied Sciences **9**, 3852 (2019).
[10]   Tabery C, Morokuma H, Sugiyama A and Page L, Evaluation of OPC Quality Using Automated Edge Placement Error Measurement with CD-SEM, International Society for Optics and Photonics, 61521F (2006).
[11]   Tanaka M, Meessen J, Shishido C, Watanabe K, Minnaert-Janssen I and Vanoppen P, CD Bias Reduction in CD-SEM Linewidth Measurements for Advanced Lithography, International Society for Optics and Photonics, 69221T (2008).
[12]   Xiao-dong Z, Bin W and Zhi-yuan Y, Journal of Measurement Science & Instrumentation **8**, 238 (2017).